

# Welding by Single Bead Test, and Rapid Heating and Cooling Structures of 13% Chromium Stainless Steel

著者	HOMMA Masao, MORITA Sougorho, YAMAYA Katsunobu
journal or publication title	Science reports of the Research Institutes, Tohoku University. Ser. A, Physics, chemistry and metallurgy
volume	17/18
page range	277-289
year	1965
URL	<a href="http://hdl.handle.net/10097/27257">http://hdl.handle.net/10097/27257</a>

# Welding by Single Bead Test, and Rapid Heating and Cooling Structures of 13% Chromium Martensitic Stainless Steel\*

Masao HOMMA, Sougorho MORITA and Katsunobu YAMAYA

*The Research Institute for Iron, Steel and Other Metals*

(Received September 16, 1965)

## Synopsis

The metallographic studies have been performed on the structures of weld metal and heat-affected zone of 13% chromium martensitic stainless steel. The heat-affected zone was obtained by single bead welding, in which a single bead 10~12cm long was put on 13% chromium stainless steel plate  $200 \times 75 \times 20\text{mm}^3$ . The isothermal austenitization diagrams (T-T-A diagram, Time-Temperature-Austenitization diagram) were determined for two specimens differently preheat-treated. The specimen was heated in a salt bath, followed by rapid quenching in water, and then T-T-A diagram was obtained from changes in hardness (Hv) and in matrix structure.

## I. Introduction

In recent years, high chromium stainless steel has come to be extensively used in many industrial plants<sup>(1)</sup>, but the metallographic investigation has not sufficiently been made in detail of the structures after rapid heating and cooling such as arc welding<sup>(2)(3)</sup>. Recently, weldment has been required for good corrosion resistance and manufacture precision, because the manufacture of the stainless steel has been very advanced.

In the present investigation, the metallographic studies have been performed on the structures and the hardness of the weld metal and the heat-affected zone of about 13% chromium martensitic stainless steel by a single bead weld method,<sup>(4)-(6)</sup> the composition of which is the most fundamental in chromium stainless steels. In order to examine the influence on the structures and the precipitations in the base metal by rapid heating and cooling, the base metal differently preheat-treated was quickly heated above  $A_{C1}$  point in the salt bath, held at an isothermal temperature for a certain time, and then quenched in water. The process of the austenitization by the isothermal treatment, i.e., isothermal austenitization

---

\* The 1212th report of the Research Institute for Iron, Steel and Other Metals.

(1) M. Hasegawa, *Stainless Steel Handbook*, Nikkan Kogyo (1959), 973.

(2) J. Cotheren and A.E. Near, *Weld. J.*, **40** (1961), 489-s.

(3) E.F. Nippes et al., *Weld. J.*, **38** (1959), 360-s.

(4) A.W. Manlove, *Weld. J.*, **20** (1941), 324-s.

(5) S.A. Herres, *Trans. ASM*, **33**(1944), 535.

(6) M. Homma, T. Wada and K. Yamaya, *J. Japan Weld. Soc.*, **29** (1960), 812.

diagram (T-T-A diagram, Time-Temperature-Austenitization diagram) was obtained from the changes in the hardness and in the matrix structures of the specimens differently preheat-treated. The nonuniformity of the matrix structures by rapid heating and cooling was determined by the T-T-A diagrams.

## II. Specimens

The base metal was synthesized in atmosphere from electrolytic iron and chromium by using a high frequency induction furnace. This base metal was cast into an iron mold in 90mm in width and 90mm in length, and then forged into a plate 75mm in width, 200mm in length and 20mm in thickness for the single bead welding test. The isothermally treated specimens were forged and then wire-drawn to 10mm in length and 1.0~1.5 mm in diameter.

Table 1. Chemical composition of the base metal and the electrode.

Kind	Chemical composition (%)						
	C	Si	Mn	P	S	Cr	Ni
Base metal	0.13	0.83	0.56	0.003	0.027	13.69	—
Electrode	0.07	0.90	1.00	0.040	0.030	13.00	0.60

The chemical compositions of the specimen are shown in Table 1. The preheat treatments of the base metal and the isothermally treated specimens were the same. The matrix structures of those specimens preheat-treated are shown in Phot. 1. The specimen shown in Phot. 1-a was subjected only to a solid solution treatment, i.e., quenched in oil after heating at 1050°C for 30 min. The matrix structure consisted almost of the martensitic phase, a small amount of  $\delta$ -ferrite being retained<sup>(7)(8)</sup> as shown in white part in the structure.

The specimen shown in Phot. 1-b was quenched in oil after heating at 1050°C for 30 min as a solid solution treatment, and after re-heating at 850°C for 4 hrs, furnace-cooled to 600°C at the rate of 50°/hr, and then air-cooled. The matrix structure of this specimen contained small precipitated carbide in  $\alpha$ -ferrite. The specimen shown in Phot. 1-c was quenched in oil after heating at 950°C for 1 hr as a solid solution treatment, and after re-heating at 700°C for 4 hrs, furnace-cooled to 600°C at the rate of 50°/hr and then air-cooled. The matrix structure was similar to that shown in Phot. 1-b.

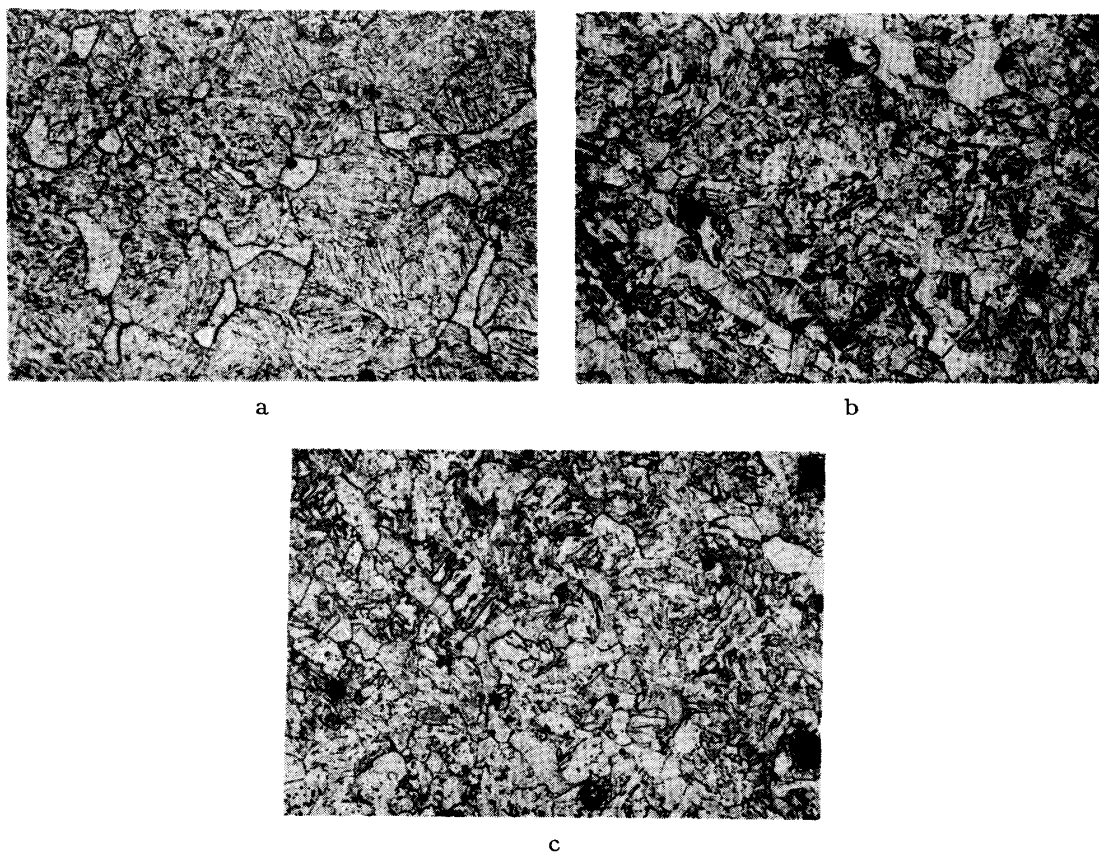
Hereafter, the specimens heat-treated like those shown in Photos. 1-a, b, and c were called respectively Cr-ST, Cr-HA, and Cr-LA.

The commercial electrode was used. This electrode was of lime titania type

(7) A.E. Nehrenberg and N.J. Harrison, Metal Progr., **60** (1951), 64.

(8) R.L. Ricket et al., Trans. ASM, **44** (1952), 138.

containing 13% chromium. The chemical compositions of the electrode are shown in Table 1 together with those of the base metal.



- a : 1050°C 30 min O.Q.  
 b : 1050°C 30 min O.Q. 850°C 4hr F.C, 600°C A.C.  
 c : 950°C 1hr O.Q. 700°C 4hr F.C, 600°C A.C.

Phot. 1. Microstructure of the base metal preheat-treated.  
 ( $\times 300$ ) etched Villela

### III. Experimental procedures

The single bead welding test was performed with A.C. welding transformer setting the welding current of 135A. The rate of deposition was about 10 cm/min, the angle of electrode inclination was about 60°C, and the single bead welding test was performed by manual welding. The single beads of 10~12 cm length were laid along the longitudinal axis of  $200 \times 75 \times 20 \text{mm}^3$  plate whose surface had been ground to flat and cleaned prior to welding to remove mill scale and other foreign matter. In the arc welding, a thermal cycling of heat-affected zone using  $200 \times 75 \times 20 \text{mm}^3$  plate was closely approximated to that of infinite plate over the temperature range of 300°C. <sup>(9)</sup><sup>(10)</sup><sup>(11)</sup> Because the cooling rate was varied by welding table, single

(9) M. Inagaki, J. Japan Weld. Soc., **27** (1958), 716.

(10) M. Inagaki, J. Japan Weld. Soc., **28** (1959), 25, 32.

(11) M. Inagaki, J. Japan Weld. Soc., **28** (1959), 25, 31.

bead welding was performed by making use of the welding table, on which were placed the mild steel bars of 13 mm  $\phi$  at intervals of 50 mm.

To determine the T-T-A diagram, the isothermal heat treatment was done, that is, the specimens were heated in the salt bath at the respective temperatures and for the respective time, and then rapidly quenched in water.<sup>(12)(13)</sup>

In obtaining the relation between the size of isothermally treated specimen and the heating and cooling rate of the heat-affected zone in the arc welding, the cooling rate was nearly the same as that of oil quenching<sup>(9)(10)</sup>. In examining the T-T-A diagrams, the cooling rate of isothermally treated specimen was approximated to that of heat-affected zone after arc welding. But it seems that the heating rate of the isothermally treated specimen by the salt bath was smaller than that of the heat-affected zone by arc welding, because the temperature of the weld metal during arc welding was higher than the temperature of the salt bath. Therefore, the size of the specimen used for the isothermal treatment had to be as small as possible, and so the size of specimen was chosen to be of 1.0~1.5 mm in diameter and 10 mm in length. As the specimen was subjected to rapid heating and cooling and the influence of binder was desired to be small, the specimen was connected with a mild steel wire binder 0.5 mm in diameter.

The hardness was measured with a micro-Vicker's hardness tester under the load of 500g.

#### IV. Experimental results and consideration

##### 1. Structures and hardness in the weldment

In the quenched state of 13% chromium stainless steel, most part of the matrix structure was composed of the martensitic phase<sup>(7)(8)</sup>. This steel was apt to break easily by repeated loading or by impact stress<sup>(14)</sup>, because of the martensitic structure. The 13% chromium stainless steel of the quenched state is hardly used on account of these characteristics<sup>(14)</sup>. As the martensitic phase is metastable at room temperature, it may be considered that the martensitic base metal shows a remarkable change in hardness and structure in the heat-affected zone by small welding heat input.

The single bead was put on the specimen Cr-ST which was transformed by solid solution treatment. Fig. 1 shows the spatial distribution of the hardness in the as-welded state. Dark marks in Fig. 1 refer to the spatial distribution of the hardness after tempering treatment, in which the weldment of the specimen was cooled to 600°C in the furnace after heating at 850°C for 4 hrs and then air-cooled.

The deposit metal showed a dendritic structure having martensitic phase. It may be considered that these structure is low carbon martensite<sup>(15)</sup> because

(12) S. Owaku and H. Akasu, J. Japan Inst. Metals, **25** (1961), 515.

(13) S. Owaku and H. Akasu, J. Japan Inst. Metals, **26** (1962), 518.

(14) M. Okamoto, *Iron and Steel as Engineering Material*, Corona-Sha (1960), 133.

(15) R. Mitsche und K.L. Maner, Arch. Eisenhüttenwes., **26** (1955), 563.

the carbon content of electrode is comparatively low. Therefore, Vicker's hardness of the deposit metal is nearly equal to that of the base metal. No crack appeared in the deposit metal and in the heat-affected zone.

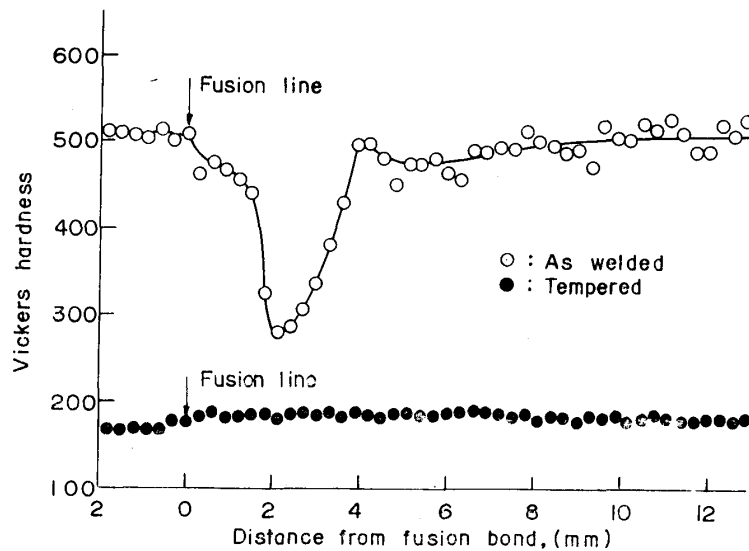
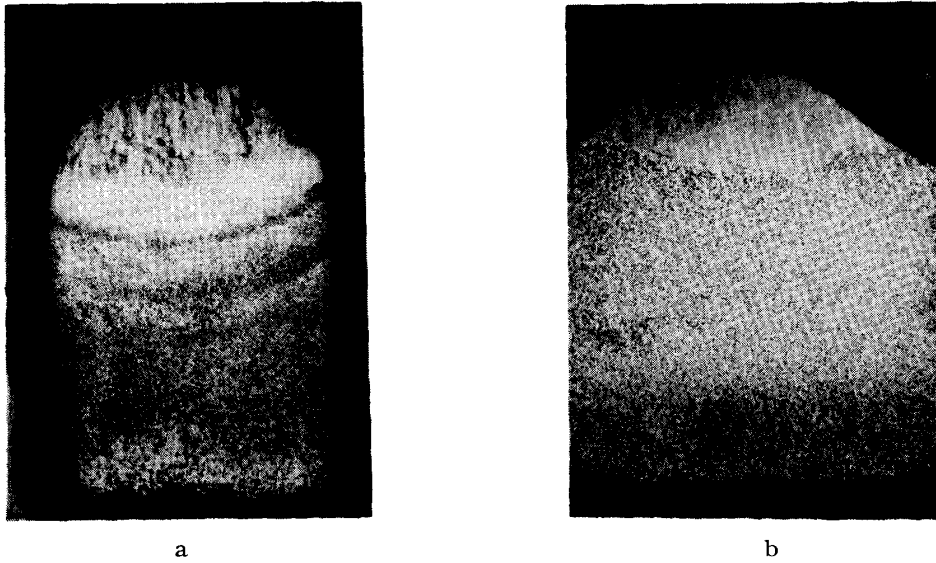


Fig. 1. Hardness of as-welded and post-heat-treated specimen Cr-ST.

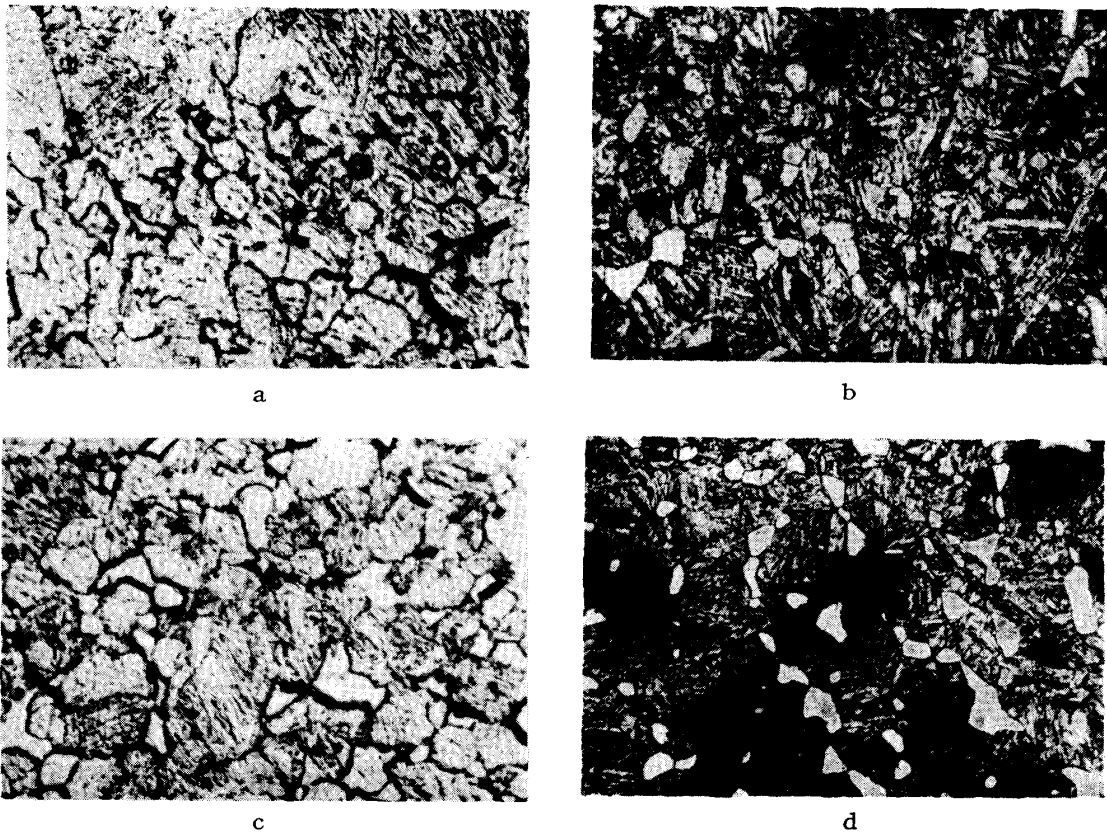
As the specimen Cr-ST was composed mainly of martensitic phase by solid solution treatment, the heat-affected zone was tempered by arc welding input energy. Therefore, the spatial distribution of the hardness in the heat-affected zone was expressed by a concave curve having a minimum point about 2 mm apart from the fusion line. From the spatial distribution of the hardness and the matrix structure in the heat-affected zone, it is clear that the left side of the minimum point in the concave hardness distribution curve, i.e., the vicinity of the fusion line may be heated above  $A_{C1}$  point by arc welding input energy. At the nearest part to the fusion line the structure in a gentle slope of the hardness distributive range (to about 1.0 mm from the fusion line) remained with an appreciable amount of  $\delta$ -ferrite, and so it is clear that this part was perfectly austenitized or imperfectly dissolved by higher arc welding input energy.

The right side of the minimum point in the curve, i.e., the detached part from the fusion line in the heat-affected zone (about from 2.0 mm to 4.0mm) was tempered, being heated up to a temperature below  $A_{C1}$  point by the arc welding input energy.

When this weldment was cooled in air at 600°C as mentioned above, the deposit metal was tempered, the hardness approaching that of the base metal. But the dendritic structure remained as it was. The heat-affected zone was tempered to the state showing somewhat higher hardness than those of the deposit metal and the base metal. The macrostructures of as-welded state and post-heat-treated weldments are shown in Phot. 2.



a : As-welded  
 b : Post-heat-treated at 850°C 4hr.F.C, 600°C A.C. after welding  
 Phot. 2. As-welded and post-heat-treated macrostructure of the specimen  
 Cr-ST( $\times 5$ ) etched Villela



a : bond                      b : 0.2 mm apart  
 c : 1.8 mm apart          d : 2.9 mm apart  
 Phot. 3. Microstructures of bond and each position apart from bond of  
 as-welded specimen Cr-ST ( $\times 300$ ) etched Villela

Phot. 3 shows the structure of the heat-affected zone of the specimen Cr-ST in as-welded state. As the nearest part to the fusion line received higher arc welding input energy in the heat-affected zone, its structure showed the martensitic phase, but an appreciable amount of  $\delta$ -ferrite remained in the martensitic structure. Little difference was shown in hardness in the range of about 1.0 mm from the fusion line in the heat-affected zone, but the coarse grained weld heat-affected structure existed within the distance about 0.4 mm from the fusion line in the heat-affected zone. For instance, this structure is shown in Photos. 3-a and b. The chromium carbide was gathered in flock in the part showing the sudden drop in the hardness. In the layer of tempered sorbitic and bainitic structures, these chromium carbides were gathered in large flock and seen in pit-corrosion by the etching of glycerin solution of mixed acid.

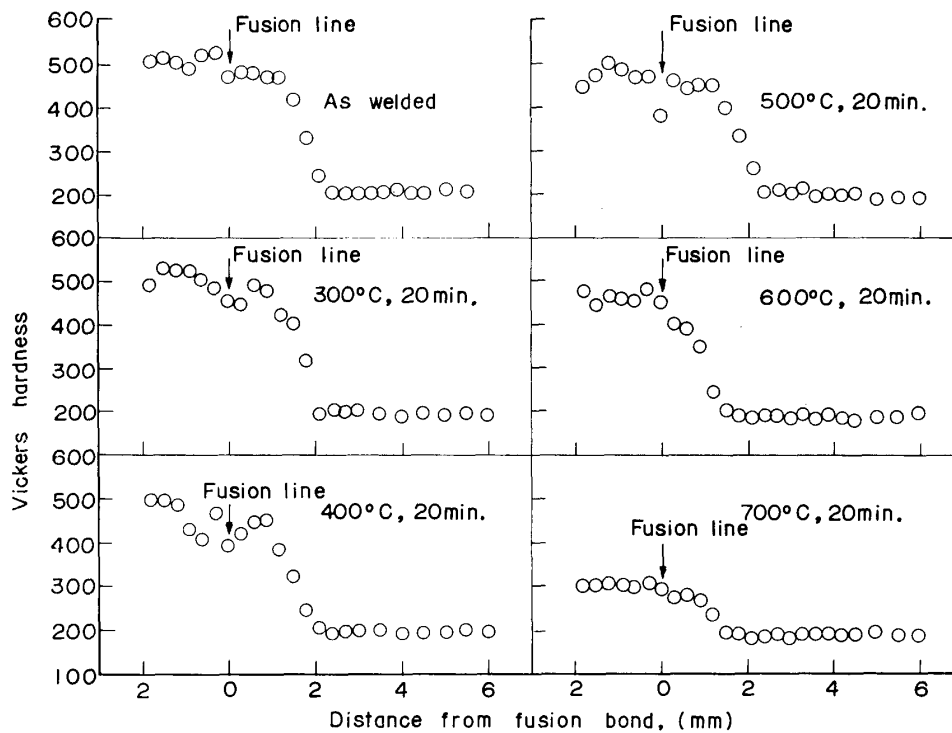


Fig. 2. Change of hardness of specimen Cr-HA.

## 2. Structure and hardness by post-heat treatment

Fig. 2 shows the spatial distribution of the hardness in the weldment of specimen Cr-HA of the as-welded state and of the post-weld states at 300°C~700°C for 20 min.

Fig. 3 shows the spatial distribution of the hardness in the weldment of specimen Cr-LA of the as-welded state and of the post-weld tempered states at 300°C~600°C for 20 min. After tempering at 300°C~600°C for 20 min, the hardness in the weldment hardly decreased. This phenomenon was in agreement



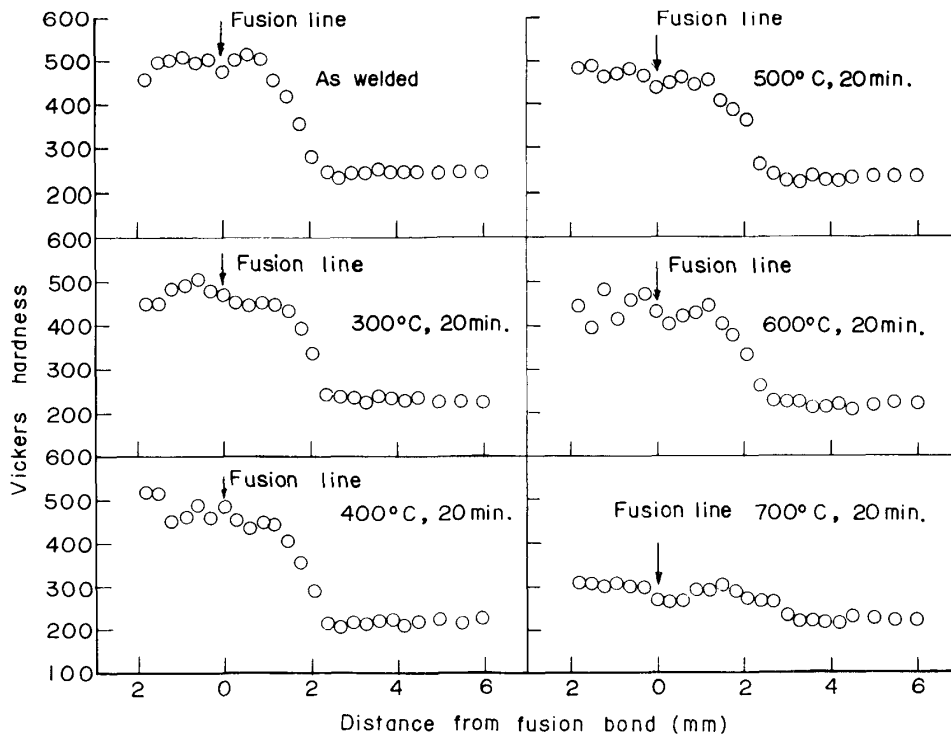
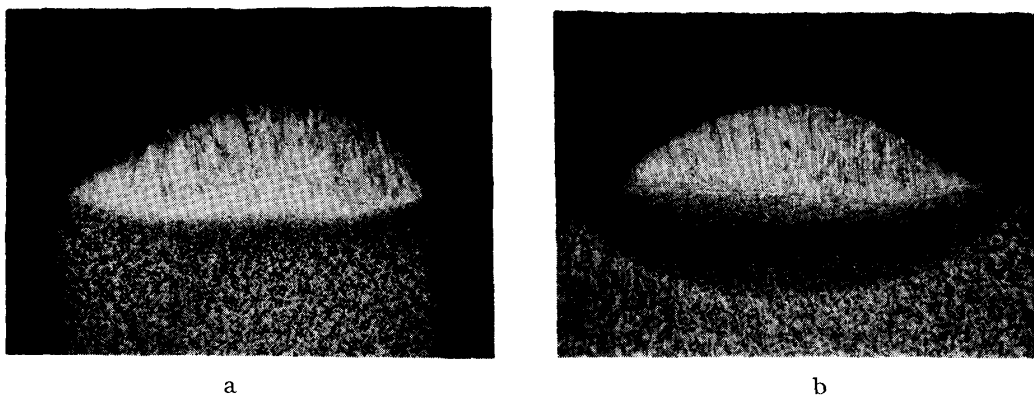


Fig. 3. Change of hardness of specimen Cr-LA.

with conventional reports on the tempering of the martensite<sup>(7)(8)(16)</sup> in carbon steel. After tempering at 700°C for 20 min, the hardness in the weldment dropped to micro-Vicker's hardness of about 300, with ferrite precipitating in the martensitic structure near the fusion range.



a : As-welded  
b : 700°C 20 min. A.C

Phot. 4. Etched figures of specimens Cr-HA and Cr-LA ( $\times 5$ ) etched Villela

Phot. 4 shows the corrosion resistance in the heat-affected zone which is etched in glycerin solution of mixed acid. In the as-welded state, the layer of the

(16) B.S. Lement et al., Trans. ASM, 46 (1954), 851.

heat-affected zone by heating at relatively low temperatures showed the corrosion resistance lower than the layer exposed to relatively high temperatures in heat-affected zone with  $\delta$ -ferrite precipitating in the martensitic phase. When the weldments were cooled in air at  $300^{\circ}\text{C}\sim 700^{\circ}\text{C}$  for 20 min, the structure in the heat-affected zone changed into tempered sorbitic and bainitic structure with the chromium carbide precipitating, and the corrosion resistance in the heat-affected zone decreased further.

### 3. Relation between temperature, hardness and structure by the isothermal treatment

The relations between temperature, hardness and structure of the base metal and the electrode were obtained to determine the T-T-A diagram. Fig. 4 shows those of the base metal and the electrode. To examine these, the specimen, after being heated at a certain temperature for 20 min in the salt bath, was quenched in water, and then the hardness was measured. The relation shown in Fig. 4 was mainly determined by the hardness. Because  $A_3$  point cannot be determined from the hardness, it cannot be made out from the curve shown in Fig. 4. But  $A_{C1}$  point is seen by a rapid rise of the hardness curve in Fig. 4<sup>(17)</sup>. It may be clear that the austenitization will begin, if the specimen is heated above the  $A_{C1}$  point.

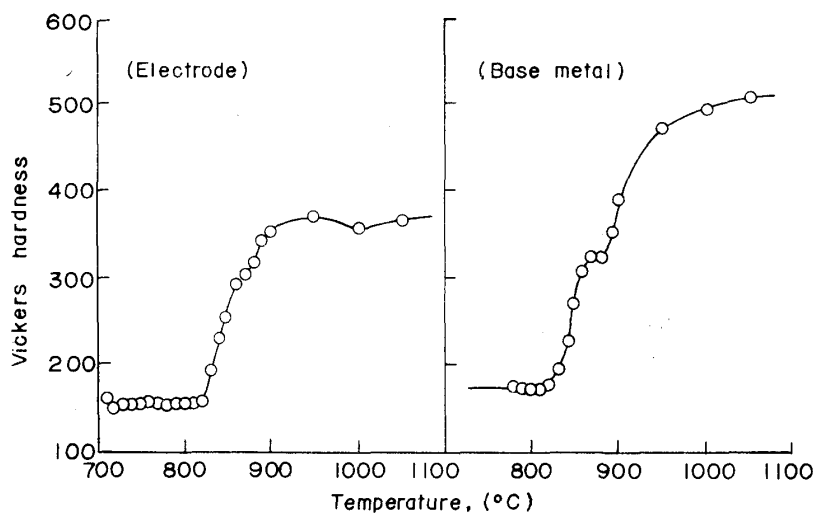


Fig. 4. Hardness of electrode and base metal heat-treated at various temperatures. (holding time, 20min)

In a pure Fe-Cr system,  $A_3$  point coincides with  $A_4$  point at about 12.4% chromium content, and the existence of the  $\gamma$ -roop is well known. Further,  $A_{C1}$  point does not exist in pure Fe-Cr system<sup>(18)</sup>. The existence of the  $\gamma$ -roop is

(17) S. Okamoto and T. Naito, *J. Japan Inst. Metals*, **24** (1960), 633.

(18) Hansen, *Constitution of Binary Alloys* (1958), 525.

greatly affected by the content of impurities such as carbon and nitrogen. If those impurities are added to Fe-Cr alloys,  $A_{C1}$  and  $A_{C3}$  points will come out<sup>(18)</sup>, and the  $A_{C1}$  point is pointed out as indicated in Fig. 4. In the high temperature range in Fig. 4, the curve of the hardness distribution shows a peak<sup>(7)</sup> and then the hardness decreases gradually with the increase of  $\delta$ -ferrite. In the high temperature range, the difference in hardness between the base metal and the electrode was influenced mainly by carbon content of these metals.

The specimen Cr-ST, 10 mm in length and 1.0~1.5 mm in diameter, was heated in the salt bath at the respective temperatures for the respective time, and then quenched in water. The relations between the time allowed to start, hardness and structure were determined. The result is shown in Fig. 5. The hardness in solid-solution-treated state was about 500 in Vicker's hardness. The higher the temperature to heat the specimen was, the further the hardness decreased. The

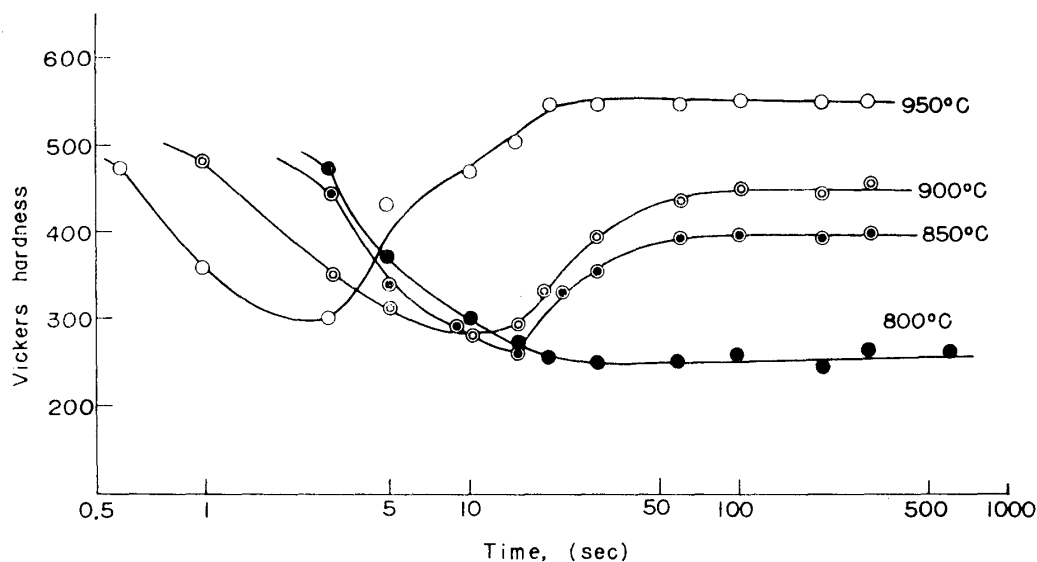


Fig. 5. Relation between hardness and holding time at various austenitizing temperatures with specimen Cr-ST.

hardness distribution showed a minimum point at a certain holding time and then the hardness increased with increasing holding time. The decrease in hardness may be considered to be due to the tempering of martensitic phase. The higher the temperature at which the specimen heated was, the faster the tempering rate became. The minimum hardness number was a little higher with higher treating temperature. The specimen treated at 800°C did not harden, and it may be considered that this temperature does not reach  $A_{C1}$  point as shown in Fig. 4.

The isothermal treatment and the size of the specimen Cr-HA were the same as those of the specimen Cr-ST. This result is shown in Fig. 6. The higher the temperature to heat specimen was, the faster the hardness increased, and the shorter the hardness reached maximum hardness number. Therefore, it may be

clear that the higher the temperature to treat specimen is, the shorter the starting and the finishing time of the austenitization becomes.

When the specimen was isothermally treated at relatively low temperature, the rise of the hardness curve took place in two steps and formed a plateau. But, when the specimen was treated at relatively high temperature, no plateau existed. Since the ferritic phase first transforms into austenitic phase and then the tempered fine chromium carbide dissolves into austenitic phase, the hardness curve shows two steps and forms the plateau with the isothermal treatment at relatively low temperature. When the specimen is isothermally treated at relatively high temperature, it may be considered that the transformation of ferrite into austenitic phase and the dissolution of tempered fine chromium carbide into austenitic phase take place simultaneously. Therefore, the plateau of the hardness curve disappears and the completion time of austenitization is shortened.

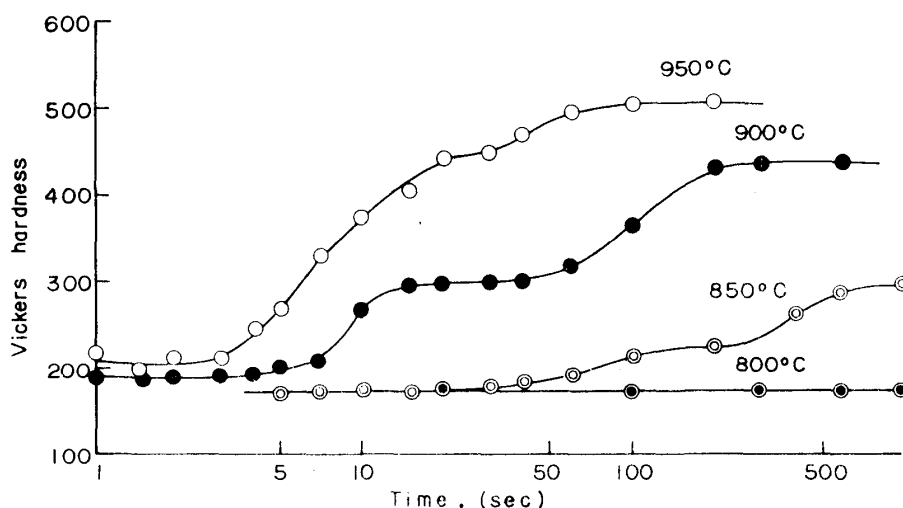


Fig. 6. Relation between hardness and holding time at various austenitizing temperatures with specimen Cr-HA.

#### 4. T-T-A diagrams

T-T-A diagrams of the specimens Cr-ST and Cr-HA are shown in Fig. 7. The start and the finish of austenitization were used to change of hardness after isothermal treatment.

The greater part of the matrix structure of the specimen Cr-ST was composed of the martensitic phase, but a little amount of  $\delta$ -ferrite remained. The martensitic phase, which was formed by shear displacement and diffusionless transformation of the elements in austenitic phase, indicates the phenomenon of tempering, when the martensitic phase is heated above the austenitization temperature.

The structure of the specimen Cr-HA mostly consisted of ferrite with precipitated fine carbide particle, because this specimen was fully tempered at the preheat treatment. Therefore, when this specimen was heated up to austenitization temperature, the structure transformed into austenitic phase with the diffusion of

fine carbide particles. It may be clear that the austenitization in specimen Cr-ST starts and finishes more rapidly than that in the specimen Cr-HA.

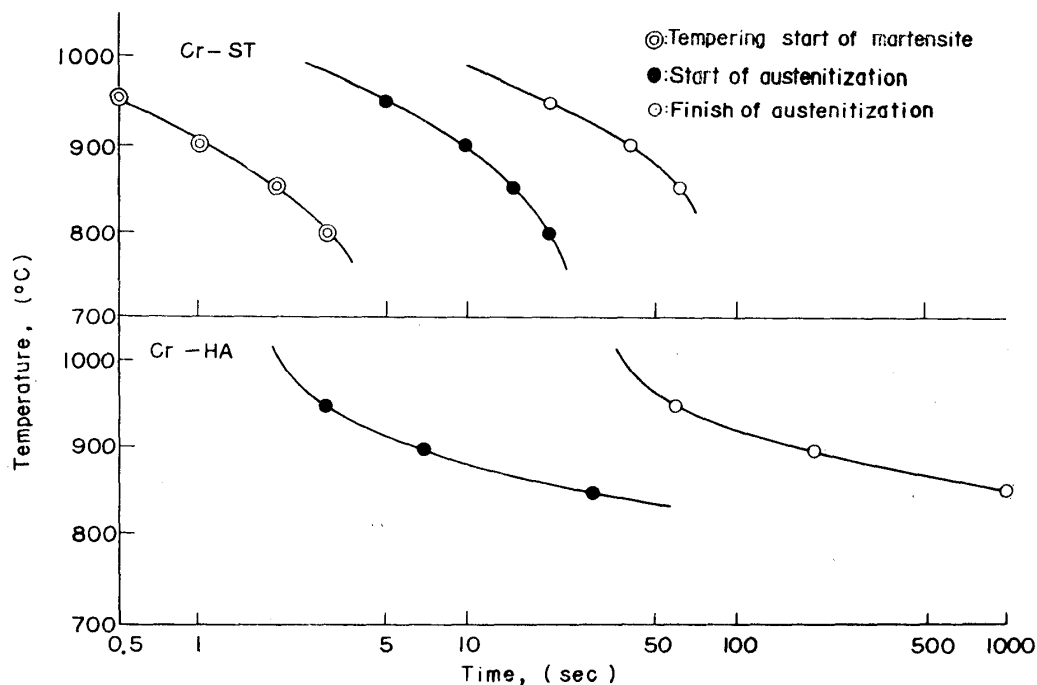


Fig. 7. T-T-A diagrams of specimens Cr-ST and Cr-HA.

### Summary

The present results may be summarized as follows:

(1) In the specimen heated at 1050°C for 30 min and then oil-quenched, the heat-affected zone is sharply divided into two parts: one is heated over  $A_{C1}$  point and the other is tempered at temperatures lower than  $A_{C1}$  point. This is characterized by hardness.

(2) If a 13% chromium martensitic stainless steel is welded by arc welding, the hardness of heat-affected zone approaches those of base metal by short time annealing at 700°C, but chromium carbide of heat-affected zone is precipitated.

(3) By rapid heating and cooling, if carbon content of 13% chromium martensitic stainless steel is different, maximum hardness is different, but  $A_{C1}$  point is nearly the same. The curve of hardness is characterized by having a peak at a certain temperature.

(4) The T-T-A diagrams were obtained with the specimens differently treated. It was clear that, in the rapid heating and quenching, if the specimens were heated up to the specified temperature, a very short holding time was sufficient for hardening.

(5) Regarding the different preheat treatments of 13% chromium martensitic stainless steel, the austenitization time of the specimen treated only by solid solutioning is shorter than that of the annealed specimen.

#### **Acknowledgement**

The authors wish to thank Mr. Y. Chiba for the performance of manual single bead welding.